INORGANIC CHEMISTRY
FRONTIERS

RESEARCH ARTICLE

View Article Online
View Journal | View Issue

Cite this: *Inorg. Chem. Front.*, 2022, **9**, 3839

A novel copper metal–organic framework catalyst for the highly efficient conversion of CO_2 with propargylic amines†

Xiao Xu, Zhentao Li, Huilin Huang, Xu Jing * and Chunying Duan

Received 30th March 2022,
Accepted 5th June 2022

DOI: 10.1039/d2qi00678b

rsc.li/frontiers-inorganic

The rapid increase in atmospheric carbon dioxide has resulted in the greenhouse effect. Hence, carbon dioxide capture and further fixation into valuable chemical products are particularly important for reducing atmospheric carbon dioxide concentrations. In this direction, a novel copper-based metal three-dimensional framework, Cu-**TSP**, was assembled from tripod ligands containing thiourea groups; this heterogeneous material can efficiently catalyze the reaction of propargylic amines and carbon dioxide to synthesize 2-oxazolidinones, and the recyclability and high conversion rates demonstrate the broad potential applications of this designed material as a π-activated catalyst in the chemical industry.

Introduction

The rapid consumption of fossil fuels has led to excessive emissions of carbon dioxide leading to increasing concentrations of carbon dioxide in the atmosphere, which is the main cause of climate warming. To alleviate the abovementioned environmental problems, a lot of work on the capture, storage and utilization of carbon dioxide has been carried out.[1–5] Strategies for converting carbon dioxide into high value-added chemicals using clean and renewable solar energy is a very promising pathway to address energy and environmental issues.[6–11] Among the environmentally friendly and atom economical reactions, the carboxyl cyclization of propargylic amines with CO_2 to generate 2-oxazolidinones has a wide range of potential applications in synthetic and medicinal chemistry.[12–15] Due to the high thermodynamic stability and kinetic inertness of CO_2, exploring highly efficient catalysts has been a central theme of research. From the perspective of industrial production, constructing heterogeneous catalysts has the advantages of easy separation and recyclability. A series of heterogeneous catalytic systems, such as immobilized organometallic species[16] and supported metal nanoparticles,[17] have been used for CO_2 chemical fixation, but their catalytic performances are still unsatisfactory in terms of stability, recyclability, turnover, *etc.*

Metal–organic frameworks are ideal heterogeneous catalysts for CO_2 chemical fixation because of their periodic, open structures, controllable pores, and highly dispersed catalytic sites.[18–21] In recent years, many silver cluster-based and cuprous cluster-based MOFs have been used for the reaction of propargylic amines with CO_2.[22–25] Although these catalysts show the special advantages of MOF catalysis with good catalytic efficiency, these catalytic systems usually require the incorporation of noble metals or harsh reaction conditions (high temperature, high pressure, and strong base). Therefore, the construction of efficient and inexpensive MOF-based catalysts for the conversion of CO_2 to oxazolidinones under mild conditions remains a big challenge at present.

By incorporating tridentate thiourea ligands, we successfully constructed a three-dimensional framework with copper as the metal center. Catalytic exploration reveals that Cu-**TSP** could efficiently catalyze the cyclization of propargylic amines with CO_2 into 2-oxazolidinones by using DBU as the base under ambient conditions (50 °C, 0.1 MPa CO_2), and the robust framework of Cu-**TSP** can be recycled at least five times without an obvious decrease in the catalytic activity (Scheme 1).

Experimental

Materials and instrumentation

All substrates were used as received from commercial suppliers unless otherwise stated. Chemicals were purchased from Sigma-Aldrich, Chempur, TCI, or Alfa Aesar. Carbon dioxide (99.995%) was purchased from the Dalian Institute of Special Gases and used as received. The ligand 2,2′,2″-(benzene-1,3,5-triyltris(ethan-1-yl-1-ylidene))tris(hydrazine-1-carbothioamide)

State Key Laboratory of Fine Chemicals, Zhang Dayu College of Chemistry, Dalian University of Technology, 116024, P. R. China. E-mail: xjing@dlut.edu.cn

†Electronic supplementary information (ESI) available. CCDC 2160451. For ESI and crystallographic data in CIF or other electronic format see DOI: https://doi.org/10.1039/d2qi00678b

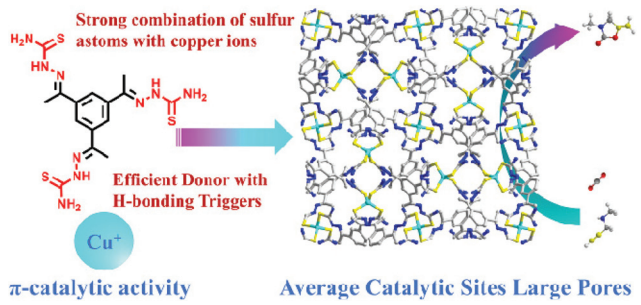

Scheme 1 Perspective views of the construction of the porous coordination polymers and the catalytic conversion of carbon dioxide with propargylic amines to oxazolidinones.

(**TSP**) was synthesized according to the previously reported procedure. ^{1}H NMR data were collected on a Varian DLG400 MHz spectrometer at ambient temperature. Peak frequencies were referenced *versus* an internal standard (TMS) for ^{1}H NMR. FT-IR spectra were recorded using KBr pellets on a JASCO FT/IR-430 spectrometer. Powder XRD diffractograms were obtained on a Rigaku D/Max-2400 X-ray diffractometer with a sealed Cu tube (λ = 1.54178 Å). IR spectra were recorded as KBr pellets on a NEXUS instrument. Thermogravimetric analyses (TGA) were performed at a ramp rate of 10 °C min^{-1} in a nitrogen flow with an SDTQ600 instrument. Confocal laser scanning microscopy micrographs were recorded using an Olympus Fluoview FV1000 with λ_{ex} = 617 nm. Liquid UV-vis spectra were recorded on a TU-1900 spectrophotometer. The solid UV-vis spectra were recorded on a Hitachi U-4100 UV-vis-NIR spectrophotometer. The microstructure and morphology observations of samples were performed with a scanning electron microscope (SEM) (HITACHI UHR FE-SEM SU8220).

Synthesis of Cu-TSP

In a glass tube, **TSP** (4.2 mg) was dissolved in DMF (2.0 mL) and then 10 mL of a DMF/CH_3CN solution (1/8 v/v) was carefully layered followed by a layer of $Cu(CH_3CN)_4BF_4$ (4.7 mg) dissolved in CH_3CN (2.0 mL). The container was covered and stored in the dark for the slow diffusion of the reactants at room temperature, to afford pale yellow crystals within 3 weeks. The catalysts were soaked in ethanol and ether for guest molecular exchange. Yield: 40% (based on Cu).

The method of catalysis by Cu-TSP

The catalytic reaction was conducted in a 10 mL Schlenk tube with the catalyst (2 mol% based on Cu, 3.7 mg for Cu-**TSP**), 0.3 mmol of propargylic amine, 0.03 mmol (10 mol%) of DBU, and 3 mL of acetonitrile as the solvent. The reaction system was purged by bubbling CO_2 for 10 min, then the reaction was sustained with 0.1 MPa CO_2 at 50 °C for 1 day. The yields were determined using ^{1}H NMR spectroscopy.

Single-crystal analysis

X-ray intensity data were recorded on a Bruker SMART APEX charge-coupled device-based diffractometer (Mo Kα radiation, λ 0.71073 Å) with the SAINT and SMART programs. The SAINT software was used in data integration and reduction. Empirical absorption correction, which was applied to the collected reflection, worked with SADABS. SHELXTL was used to solve the structures in direct methods, which was refined on F^2 by the full-matrix least-squares method using the SHELXL-97 program.[26–28]

Results and discussion

Synthesis and structure of Cu-TSP

The **TSP** ligand was prepared from a Schiff base reaction of thiosemicarbazide and 1,3,5-triacetylbenzene with a high yield. Slow diffusion of $Cu(MeCN)_4BF_4$ into a **TSP** solution produces Cu-**TSP** (Fig. 1). Single crystal X-ray crystallographic study reflected that Cu-**TSP** crystallizes in a cubic crystal system with a space group of I-43d. Each Cu atom coordinated with four sulfur atoms from four different ligands forming a distorted tetrahedral coordination configuration, with an average Cu–S distance of 2.325 Å. (Fig. 1a and b). The absence of any counterions implies that the C=S and C–N(H) bonds were all transformed into C–S and C=N bonds, respectively, *via* the loss of the imine protons during the coordination of the metal ions. The measured C–S, C–N, and N–N bond distances (Fig. S1–S3†) are all in the normal range of single- and double-bond lengths, suggesting extensive electron delocalization over the entire ligand skeleton.[29,30] This opening configuration of Cu sites facilitates π-interactions of Cu atoms with substrates containing unsaturated triple C–C bonds. Cu centers are regarded as connection nodes that consolidate the three-dimensional frameworks with tripodal thiourea-functionalized ligand linkers. Two types of pores are observed in this structure (Fig. 1c). The assembly of three Cu ions and **TSP** ligands form a macrocycle that exhibits a triangular window

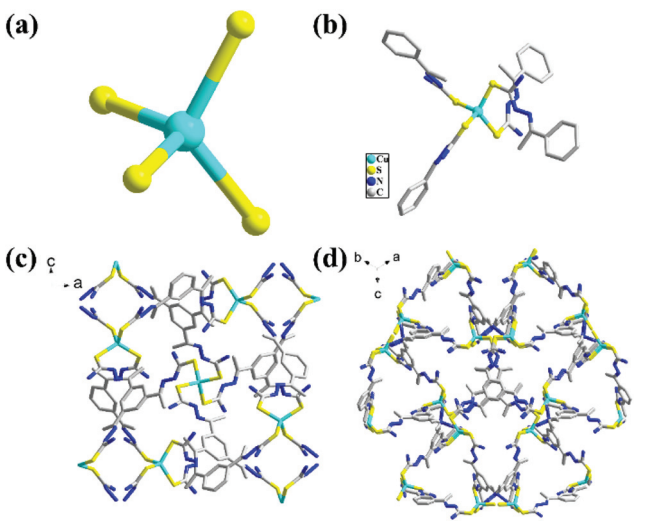

Fig. 1 (a) Distorted tetrahedral coordinating configuration of the Cu atom; (b) connecting configuration between ligands and Cu atoms; (c) view of the 3D structure along the b direction of Cu-**TSP**; and (d) represented cavities in the packing mode of Cu-**TSP**.

with dimensions of 13.6 × 13.6 Å^2 (Fig. 1d), which is large enough to absorb substrate molecules and provide the possibility of catalyzing the transformation of alkyne derivatives. On the surface of the Cu–S SBUs, there are abundant H-bond donors (–NH_2) and H-bonding acceptors (C=N– and sulfur). These hydrogen bond donors and acceptors provide potential hydrogen bonding sites during the catalytic reaction and participate in the capture and cooperative activation of reactant molecules in the pores.[31]

Characterization experiments

As obviously displayed in Fig. 2, the thermogravimetry analysis curve of the freshly synthesized Cu-**TSP** demonstrated a slow weight loss of 7% below 170 °C, corresponding to the loss of acetonitrile and DMF molecules. It indicated that the framework of Cu-**TSP** was stable below 170 °C (Fig. 2b). The characteristic diffraction patterns of the prepared Cu-**TSP** are similar to those simulated from the single crystal data of Cu-**TSP** (Fig. 2a). XPS spectra revealed that the oxidation states of Cu(I) ions in the Cu-**TSP** remained stable (Fig. 2c). The elemental mapping indicated the uniform distribution of the N, S, and Cu elements in Cu-**TSP** (Fig. 2d). The above results suggested the good purity and stability of the framework.

Although the nitrogen adsorption isotherm of Cu-**TSP** showed a limited amount of N_2 adsorption capacity at 77 K (Fig. S11†), the pore size of Cu-**TSP** was calculated to be 0.573 nm and the total volume of pores as 4 × 10^{-3} cm^3 g^{-1} by carbon dioxide adsorption (Fig. S12 and S13†). The dye uptake study was performed by soaking Cu-**TSP** in a methanol solution containing the dye malachite green, UV-vis spectra demonstrated that Cu-**TSP** could absorb 13% malachite green based on the crystal weight (Fig. 3d and Table S2†). Depth-scanning confocal laser scanning microscopy of the dye-adsorbed crystals revealed a strong green fluorescence emission that could be attributable to malachite green. The uniform distribution of the dye molecules throughout the crystals suggested that the dyes deeply penetrate the channels instead of remaining on the external surface (Fig. 3a and b). These results indicated that Cu-**TSP** had enough pores and a good ability to adsorb molecules of suitable sizes.[32,33]

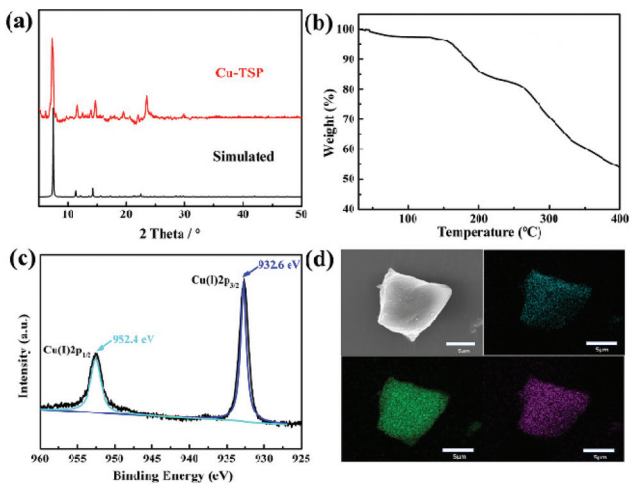

Fig. 2 (a) Simulated and experimental PXRD pattern of Cu-**TSP**; (b) the TGA curve of Cu-**TSP**; (c) the XPS spectra of Cu(I) ions in Cu-**TSP**; and (d) the HAADF-STEM images and the corresponding elemental mappings of Cu-**TSP**, N (blue), and S (green), Cu (purple), respectively.

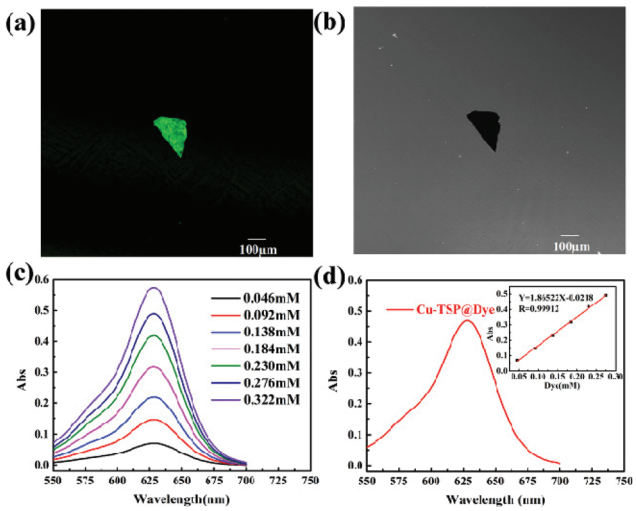

Fig. 3 (a and b) Confocal laser-scanning microscopy, dark field (a) and light field (b). (c) The UV-vis spectrum of different concentrations of malachite green dye. (d) The UV-vis absorption spectra of released malachite green from Cu-**TSP**. The standard linear relationship between the absorption and the concentration.

Carboxylation of propargylic amines with CO_2

The excellent chemical stability and highly dispersed active metal center in Cu-**TSP** could deliver high activity in catalytic reactions. Herein, the cyclization of propargylic amines with CO_2 was selected as a model reaction to examine its catalytic properties (Table 1). This reaction is very scientifically significant, and the resulting products of 2-oxazolidinones are widely used in many drugs. First, we selected

Table 1 Control experiments for the catalytic carboxylation of propargylic amines with CO_2

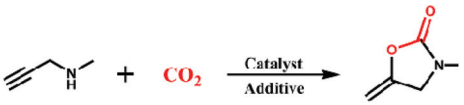

Entry	Catalyst	Base	Yield (%)
1	L	DBU	<1
2	None	DBU	0
3	L + $Cu(CH_3CN)_4BF_4$	DBU	47
4	$Cu(CH_3CN)_4BF_4$	DBU	46
5	Cu-**TSP**	DBU	99
6	Cu-**TSP**	None	3
7[a]	Cu-**TSP**	DBU	0

Reaction conditions: 1a (0.3 mmol), 1 mol% of the catalyst (based on Cu), 0.03 mmol (10 mol%) of DBU, CH_3CN (3 mL), 50 °C, 24 h, CO_2 (balloon). [a] N_2 atmosphere. The yields were determined using ^{1}H NMR spectroscopy.

N-methylpropargylamine (1a) as the model substrate to investigate the catalytic activity of Cu-**TSP**. The reaction was conducted in the presence of compound Cu-**TSP** and DBU in CH_3CN. Interestingly, Cu-**TSP** as the catalyst exhibits good catalytic activity, the corresponding product of oxazolidinones was obtained in 99% yield at 50 °C and CO_2 under atmospheric pressure for 24 h (Table 1, entry 5). In the control experiments, no detectable conversion occurred in the absence of the catalyst, and DBU itself was ineffective under the given reaction conditions (Table 1, entry 2). To explore in-depth the catalytic activity of each component in Cu-**TSP** for this reaction, ligand **TSP** was first studied, while no products could be observed (Table 1, entry 1), $Cu(CH_3CN)_4BF_4$ gave 47% yield (Table 1, entry 3). The simple mixture of $Cu(CH_3CN)_4BF_4$ and ligand **TSP** affords 46% conversion under the same reaction conditions (Table 1, entry 4). Subsequently, we also investigated the influence of a base on the reaction. The results revealed that only a 3% yield of the product can be obtained without adding any base (Table 1, entry 6). In addition, we found that the product could not be generated under a N_2 atmosphere (Table 1, entry 7). The above control experiments showed that Cu-**TSP**, DBU and CO_2 are all essential for the reaction.

As is shown in Fig. 4d, the removal of Cu-**TSP** by filtration after 4 h shuts down the reaction, and only 4% additional yield was obtained after another 20 h under the same reaction conditions (Fig. 4c), indicating that Cu-**TSP** was a true heterogeneous catalyst in the catalytic system. Additionally, recyclability is very important in industrial production, and Cu-**TSP** could be easily separated from the reaction system by filtration. Therefore, the recyclable performance of Cu-**TSP** was studied in detail. Cu-**TSP** can be recycled at least five times without an obvious decrease in the catalytic activity (Fig. 4d). Moreover, the PXRD patterns and IR spectra of the reused crystals did not exhibit any change (Fig. S4 and S5†), ICP-OES analysis of the reaction filtrate showed only a trace amount of Cu species (<0.2%), further confirming the high robustness and good reusability of Cu-**TSP**. All of these results suggested that Cu-**TSP** possesses potential application prospects in industrial production.

To test whether Cu-**TSP** could adsorb the substrate, the synthesized Cu-**TSP** was immersed in acetonitrile solution containing *N*-(4-nitrobenzyl)prop-2-yn-1-amine (4a) for 24 h. The crystalline powder was filtered, washed with acetonitrile and dried in air, and then ^{1}H NMR and IR spectra were acquired. The ^{1}H NMR of 4a-impregnated crystals (denoted Cu-**TSP**@4a) showed that Cu-**TSP** adsorbed approximately an 0.8 mole ratio of 4a per copper node (Fig. 4b). The IR spectrogram showed a new C≡C stretching vibration at 2837 cm^{-1}, while the peak of the C≡C bond of free 4a was at 2845 cm^{-1} (Fig. 4a). It demonstrated that the substrate could be absorbed by the pores of Cu-**TSP** and interact with Cu-**TSP**.[34]

Given the high catalytic activity of Cu-**TSP** in the cycloaddition of 1a with CO_2, we further explore its generality by using various propargylic amines, and the results are listed in Table 2. To our delight, many different *N*-alkyl- or *N*-aryl-sub-

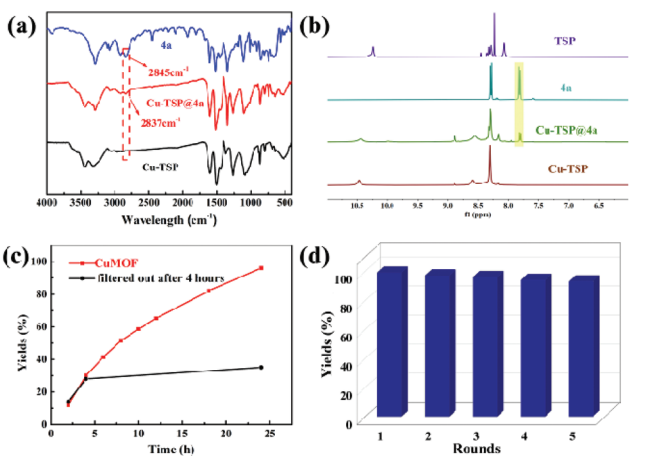

Fig. 4 (a) IR spectra of Cu-**TSP** impregnated with propargylic amine (Cu-**TSP**@4a, red); free Cu-**TSP** (black); free propargylic amine (4a, blue); (b) ^{1}H NMR spectra of the crystals of **TSP**, 4a, Cu-**TSP**, and Cu-**TSP**@4a (digested in DMSO-d_6); and (c) catalytic traces of cyclization performed under optimal conditions with the catalyst Cu-**TSP** filtered after 4 h. (d) Recycling experiments at each run.

Table 2 Catalytic results for the cycloaddition of CO_2 with different propargylic amines

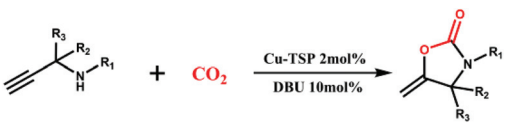

Entry	Substrates	Products	Yield (%)
1			99
2	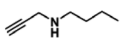	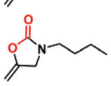	94
3	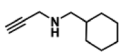	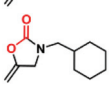	97
4	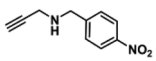	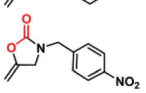	87
5	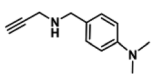	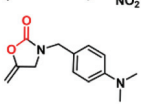	62
6	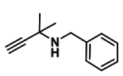	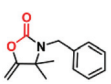	66
7	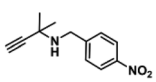	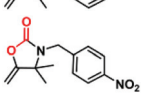	44
8	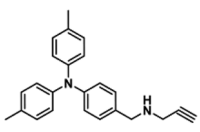	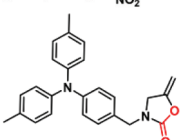	Trace

Reaction conditions: propargylic amine (0.3 mmol), 2 mol% of the catalyst (based on Cu), 0.03 mmol (10 mol%) of DBU, CH_3CN (3 mL), 50 °C, 24 h, CO_2 (balloon). The yields were determined using ^{1}H NMR spectroscopy.

stituted terminal propargylic amines (Table 2, entries 1–3 and 4) could afford the corresponding products in high yields (87–99%) under the optimal reaction conditions. Notably, propargylic amine derivatives bearing electron-donating groups on the *N*-benzyl moiety (Table 2, entry 5) provide the target products in lower yields. Moreover, the addition of the methyl group which increases the steric hindrance did reduce the yield (Table 2, entries 6 and 7). In addition, we found that the propargylic amine substrates 8a with oversized substituents are almost completely unconverted. In particular, a significant decrease in yields was observed, which suggested that the cycloaddition transformation was highly dependent on the molecular size of propargylamine derivatives.

Conclusions

In summary, we developed our previously reported synthetic methodology for the design and synthesis of Cu–S-based porous frameworks. A new Cu–S-based porous framework with distorted tetrahedrally coordinated Cu centers as connecting nodes and tripodal thiourea-functionalized ligands were synthesized and used in π-catalytic transformation with moderate to good yields of various propargylic amine derivatives. The strong Cu–S bond provided enough chemical stability, the multiple hydrogen-bonding sites on the ligands enhanced the interaction between frameworks and reactants. The large pores and appropriate coordination of the Cu centers enabled an efficient catalytic transformation to occur under mild reaction conditions. More importantly, Cu-**TSP** could be reused at least five times without obvious catalytic activity loss. This is a noble-metal-free MOF catalyst that can effectively catalyze the cyclization of propargylic amines with CO_2 under mild reaction conditions. This work will be helpful for the design of efficient MOF catalysts for CO_2 conversion.

Conflicts of interest

There are no conflicts to declare.

Acknowledgements

This work was supported by the National Natural Science Foundation of China (No. 21971030, 21890381 and 21820102001).

Notes and references

1 H. Lyu, O. I. F. Chen, N. Hanikel, M. I. Hossain, R. W. Flaig, X. Pei, A. Amin, M. D. Doherty, R. K. Impastato, T. G. Glover, D. R. Moore and O. M. Yaghi, Carbon dioxide capture chemistry of amino acid functionalized metal-organic frameworks in humid flue gas, *J. Am. Chem. Soc.*, 2022, **144**, 2387–2396.

2 A. C. Forse, P. J. Milner, J. H. Lee, H. N. Redfearn, J. Oktawiec, R. L. Siegelman, J. D. Martell, B. Dinakar, L. B. Porter-Zasada, M. I. Gonzalez, J. B. Neaton, J. R. Long and J. A. Reimer, Elucidating CO2 chemisorption in diamine-appended metal-organic frameworks, *J. Am. Chem. Soc.*, 2018, **140**, 18016–18031.

3 M. Ozkan, A. A. Akhavi, W. C. Coley, R. Shang and Y. Ma, Progress in carbon dioxide capture materials for deep decarbonization, *Chem*, 2022, **8**, 141–173.

4 Y. H. Luo, L. Z. Dong, J. Liu, S. L. Li and Y. Q. Lan, From molecular metal complex to metal-organic framework: The CO2 reduction photocatalysts with clear and tunable structure, *Coord. Chem. Rev.*, 2019, **390**, 86–126.

5 R. L. Siegelman, E. J. Kim and J. R. Long, Porous materials for carbon dioxide separations, *Nat. Mater.*, 2021, **20**, 1060–1072.

6 W. Wang, S. P. Wang, X. B. Ma and J. L. Gong, Recent advances in catalytic hydrogenation of carbon dioxide, *Chem. Soc. Rev.*, 2011, **40**, 3703–3727.

7 A. Tortajada, F. Julia-Hernandez, M. Borjesson, T. Moragas and R. Martin, Transition-metal-catalyzed carboxylation reactions with carbon dioxide, *Angew. Chem., Int. Ed.*, 2018, **57**, 15948–15982.

8 J. Zhang, B. An, Z. Li, Y. Cao, Y. Dai, W. Wang, L. Zeng, W. Lin and C. Wang, Neighboring Zn-Zr sites in a metal-organic framework for CO2 hydrogenation, *J. Am. Chem. Soc.*, 2021, **143**, 8829–8837.

9 W. Shi, Y. Quan, G. Lan, K. Ni, Y. Song, X. Jiang, C. Wang and W. Lin, Bifunctional metal-organic layers for tandem catalytic transformations using molecular oxygen and carbon dioxide, *J. Am. Chem. Soc.*, 2021, **143**, 16718–16724.

10 E. Pugliese, P. Gotico, I. Wehrung, B. Boitrel, A. Quaranta, M. H. Ha-Thi, T. Pino, M. Sircoglou, W. Leibl, Z. Halime and A. Aukauloo, Dissection of light-induced charge accumulation at a highly active iron porphyrin: Insights in the photocatalytic CO2 reduction, *Angew. Chem.*, 2022, **61**, 17530–17536.

11 R. Ma, L. N. He and Y. B. Zhou, An efficient and recyclable tetraoxo-coordinated zinc catalyst for the cycloaddition of epoxides with carbon dioxide at atmospheric pressure, *Green Chem.*, 2016, **18**, 226–231.

12 P. Brunel, J. Monot, C. E. Kefalidis, L. Maron, B. Martin-Vaca and D. Bourissou, Valorization of CO2: Preparation of 2-oxazolidinones by metal-ligand cooperative catalysis with SCS indenediide Pd complexes, *ACS Catal.*, 2017, **7**, 2652–2660.

13 S. Ghosh, R. A. Molla, U. Kayal, A. Bhaumik and S. M. Islam, Ag NPs decorated on a COF in the presence of DBU as an efficient catalytic system for the synthesis of tetramic acids via CO2 fixation into propargylic amines at atmospheric pressure, *Dalton Trans.*, 2019, **48**, 4657–4666.

14 S. L. Hou, J. Dong, X. L. Jiang, Z. H. Jiao and B. Zhao, A noble-metal-free metal-organic framework (MOF) catalyst for the highly efficient conversion of CO2 with propargylic alcohols, *Angew. Chem., Int. Ed.*, 2019, **58**, 577–581.

15 C. S. Cao, S. M. Xia, Z. J. Song, H. Xu, Y. Shi, L. N. He, P. Cheng and B. Zhao, Highly efficient conversion of propargylic amines and CO2 catalyzed by noble-metal-free

Zn116 nanocages, *Angew. Chem., Int. Ed.*, 2020, **59**, 8586–8593.

16 A. Alvarez, A. Bansode, A. Urakawa, A. V. Bavykina, T. A. Wezendonk, M. Makkee, J. Gascon and F. Kapteijn, Challenges in the greener production of formates/formic acid, methanol, and DME by heterogeneously catalyzed CO2 hydrogenation processes, *Chem. Rev.*, 2017, **117**, 9804–9838.

17 C. Calabrese, F. Giacalone and C. Aprile, Hybrid catalysts for CO2 conversion into cyclic carbonates, *Catalysts*, 2019, **9**, 325–355.

18 A. L. Gu, Y. X. Zhang, Z. L. Wu, H. Y. Cui, T. D. Hu and B. Zhao, Highly efficient conversion of propargylic alcohols and propargylic amines with CO2 activated by noble-metal-free catalyst Cu2O@ZIF-8, *Angew. Chem.*, 2022, **61**, 14817–14827.

19 Z. Wu, X. Lan, Y. Zhang, M. Li and G. Bai, Copper(I) iodide cluster-based lanthanide organic frameworks: synthesis and application as efficient catalysts for carboxylative cyclization of propargyl alcohols with CO2 under mild conditions, *Dalton Trans.*, 2019, **48**, 11063–11069.

20 K. Chen and C. D. Wu, Designed fabrication of biomimetic metal-organic frameworks for catalytic applications, *Coord. Chem. Rev.*, 2019, **378**, 445–465.

21 Y. S. Kang, Y. Lu, K. Chen, Y. Zhao, P. Wang and W. Y. Sun, Metal-organic frameworks with catalytic centers: From synthesis to catalytic application, *Coord. Chem. Rev.*, 2019, **378**, 262–280.

22 Z. Chang, X. Jing, C. He, X. Liu and C. Duan, Silver clusters as robust nodes and pi-activation sites for the construction of heterogeneous catalysts for the cycloaddition of propargylamines, *ACS Catal.*, 2018, **8**, 1384–1391.

23 M. Zhao, S. Huang, Q. Fu, W. Li, R. Guo, Q. Yao, F. Wang, P. Cui, C. H. Tung and D. Sun, Ambient chemical fixation of CO2 using a robust Ag27 cluster-based two-dimensional metal-organic framework, *Angew. Chem., Int. Ed.*, 2020, **59**, 20031–20036.

24 R. Das and C. M. Nagaraja, Highly efficient fixation of carbon dioxide at rt and atmospheric pressure conditions: Influence of polar functionality on selective capture and conversion of CO2, *Inorg. Chem.*, 2020, **59**, 9765–9773.

25 A. L. Gu, W. T. Wang, X. Y. Cheng, T. D. Hu and Z. L. Wu, Non-noble-metal metal-organic-framework-catalyzed carboxylative cyclization of propargylic amines with atmospheric carbon dioxide under ambient conditions, *Inorg. Chem.*, 2021, **60**, 13425–13433.

26 *SMART Data collection software (version 5.629)*, Bruker AXS Inc., Madison, WI, 2003.

27 *SAINT Data reduction software (version 6.45)*, Bruker AXS Inc., Madison, WI, 2003.

28 *Sheldrick, G. M. SHELXTL97 Program for crystal structure solution*, University of Göttingen, Göttingen, Germany, 1997.

29 Y. Zhao, D. Guo, Y. Liu, C. He and C. Duan, A mixed-valence (FeII)2(FeIII)2 square for molecular expression of quantum cellular automata, *Chem. Commun.*, 2008, **44**, 5725–5727.

30 X. Jing, C. He, Y. Yang and C. Duan, A metal-organic tetrahedron as a redox vehicle to encapsulate organic dyes for photocatalytic proton reduction, *J. Am. Chem. Soc.*, 2015, **137**, 3967–3974.

31 T. M. McDonald, J. A. Mason, X. Kong, E. D. Bloch, D. Gygi, A. Dani, V. Crocella, F. Giordanino, S. O. Odoh, W. S. Drisdell, B. Vlaisavljevich, A. L. Dzubak, R. Poloni, S. K. Schnell, N. Planas, K. Lee, T. Pascal, L. F. Wan, D. Prendergast, J. B. Neaton, B. Smit, J. B. Kortright, L. Gagliardi, S. Bordiga, J. A. Reimer and J. R. Long, Cooperative insertion of CO2 in diamine-appended metal-organic frameworks, *Nature*, 2015, **519**, 303–308.

32 X. Zhao, M. Zheng, X. Gao, J. Zhang, E. Wang and Z. Gao, The application of MOFs-based materials for antibacterials adsorption, *Coord. Chem. Rev.*, 2021, **440**, 213970–213986.

33 P. Brandt, S. H. Xing, J. Liang, G. Kurt, A. Nuhnen, O. Weingart and C. Janiak, Zirconium and aluminum MOFs for low-Pressure SO2 adsorption and potential separation: Elucidating the effect of small pores and NH2 groups, *ACS Appl. Mater. Interfaces*, 2021, **13**, 29137–29149.

34 H. Huang, X. Jing, B. Zhong, C. Meng and C. Duan, Cuprous cluster-based coordination sheets as photocatalytic regulators to activate oxygen, benzoquinone, and thianthrenium salts, *ACS Appl. Mater. Interfaces*, 2021, **13**, 58498–58507.

